frontiers in Environmental Science

ORIGINAL RESEARCH
published: 04 February 2022
doi: 10.3389/fenvs.2021.812039

Study of Variations in Mass Absorption Efficiency of Elemental Carbon Influenced by Different Measurement Techniques and Vehicle Emission

Dong Chen[1,2], *Zhaojin An*[2], *Qiuyue Zhao*[1], *Sijia Xia*[1], *Li Li*[1] *and Miao Guan*[3]*

[1]*Jiangsu Key Laboratory of Environmental Engineering, Jiangsu Provincial Academy of Environmental Science, Nanjing, China,*
[2]*State Key Laboratory of Pollution Control and Resource Reuse, School of the Environment, Nanjing University, Nanjing, China,*
[3]*Jiangsu Key Laboratory for Biodiversity and Biotechnology, College of Life Sciences, Nanjing Normal University, Nanjing, China*

An inter-comparison study of mass absorption efficiency (MAE) of elemental carbon (EC) by different sampling modes and measurements was conducted at the School of the Environment (SE) and Station for Observing Regional Processes of the Earth System (SORPES) in Nanjing from November 2015 to October 2016. Compared with offline sampling, the underestimation in MAE of online sampling was mainly due to the decreased optical attenuation (ATN) from the losing EC, and the difference in MAEs of the two types of sampling was greatly influenced by secondary organic aerosol (SOA) formation. Based on five temperature protocols, which include four NIOSH-derived protocols and one IMPROVE-A protocol, dependence of MAE on the temperature protocol was investigated. The main reason for the change in MAE estimation was the difference in EC determination. The result showed that low peak inert mode temperature (T_{peak}) produced a small amount of pyrolysis carbon, and this carbon fraction was typically classified as organic carbon (OC), resulting in overestimation of EC and thereby underestimation of MAE. In order to study the influence of vehicle emission of highway on MAE values of EC, the simultaneous observation at SE and SORPES was conducted. The mean MAE of SE was 8.5% lower than that of SORPES. EC concentration was estimated to decrease by 0.13 μg/m^3 with an increment distance of 100 m. Good correlation was found between the differential ATN for the two sites and the proportion of secondary organic carbon (SOC) at SORPES (R^2 = 0.71). These results indicated that high MAE at SORPES was expected to be relevant with the dry deposition of EC from vehicle emission and the lensing effect by SOA coating.

Keywords: mass absorption efficiency, black carbon, elemental carbon, temperature protocol, vehicle emission

OPEN ACCESS

Edited by:
Dantong Liu,
Zhejiang University, China

Reviewed by:
Caiqing Yan,
Shandong University, China
Yunfei Wu,
Institute of Atmospheric Physics (CAS), China

***Correspondence:**
Miao Guan
xiaoniao8911@126.com

Specialty section:
This article was submitted to Atmosphere and Climate, a section of the journal Frontiers in Environmental Science

Received: *09 November 2021*
Accepted: *13 December 2021*
Published: *04 February 2022*

Citation:
Chen D, An Z, Zhao Q, Xia S, Li L and Guan M (2022) Study of Variations in Mass Absorption Efficiency of Elemental Carbon Influenced by Different Measurement Techniques and Vehicle Emission. Front. Environ. Sci. 9:812039. doi: 10.3389/fenvs.2021.812039

INTRODUCTION

Black carbon (BC) in carbonaceous aerosol originates mainly from incomplete combustion of biomass and fossil fuels, and plays a vital role in regional radiation balance and global climate change through its light absorption characteristics (Jacobson, 2001; Bond et al., 2013). In the climate science field, elemental carbon (EC) was usually considered as the mass-based proxy for BC when evaluating the mass absorption efficiency (MAE) (Chen et al., 2017a; Cheng et al., 2017; Zhao et al., 2017).

MAE is a critical optical parameter for evaluating the light absorption ability of EC (Bond and Bergstrom, 2006); it closely links the optical properties and chemical concentration of EC. MAE

exhibited distinct spatiotemporal variation in atmospheric environment. In winter, MAE in Beijing, Shanghai, Xi'an, and Jinan (measured at 632, 678, 870, 678 nm, respectively) were estimated at 8.5, 10.0, 7.6, and 9.0 m^2/g, respectively (Cheng et al., 2011a; Wang et al., 2014; Han et al., 2015; Chen et al., 2017a). Our previous study showed that MAE values (measured at 678 nm) varied from 3.4 to 19.1 m^2/g in Nanjing in different seasons (Chen et al., 2019). A similar situation was observed in nine regional background sites in Europe with MAE values ranging from 4.55 to 26.2 m^2/g (measured at 637 and 880 nm) (Zanatta et al., 2016). MAE reported in the previous studies varied dramatically depending on source types (e.g., vehicle emission, biomass burning, and secondary aerosol formation) (Liu et al., 2017; Sun et al., 2021; Wang et al., 2021). Compared with MAEs at three sites in Nanjing, our previous study found that high MAE value at an industrial site MAE was mainly attributed to the lensing effect by secondary organic aerosol (SOA) coating (Chen et al., 2019). Shen et al. (2013) showed that MAE from the wood combustion was significantly lower than those of the other fuels. Current studies on MAE are typically based on offline sampling with temporal resolution of 1 day (Cheng et al., 2011b; Shen et al., 2013; Wang et al., 2014; Chen et al., 2019) and, thus, missed important information of dynamic evolution of MAE within a day. Instead, online sampling and analysis methods with high temporal resolution can further investigate the dynamic variation of MAE with the change in source contribution during typical pollution periods. In the MAE estimation, MAE is largely related to EC concentration, which is generally determined by thermal/optical method. Temperature protocol is an important factor influencing the concentrations of carbonaceous components during the measurement process (Chen and He, 2015). IMPROVE (Interagency Monitoring of Protected Visual Environments), NIOSH (National Institute for Occupational Safety and Health), and several modified temperature protocols of NIOSH were currently used in OCEC analysis in previous studies (Watson et al., 2005; Wu et al., 2012), and the discrepancy of these protocols were mainly reflected in the difference of temperature platform and residence time (Watson et al., 2005). There were many methods to collect EC samples and to analyze MAE values at present, while a few studies had focused on the large variance of MAE caused by the multiple sampling and measurements.

Vehicle emission (especially diesel vehicles) is considered to be the most important anthropogenic source for EC emissions (Zhao et al., 2019). Highway is the main traffic channel between cities and regions, and the proportion of diesel vehicles on expressways is much higher than that on ordinary highways (Wen et al., 2019; Abdull et al., 2020). Previous studies had shown that EC concentration at manual toll collection (MTC) lanes in highways was much higher than the concentration in ambient atmosphere (Cui et al., 2015; Chen et al., 2017a). Besides, a previous study found that the MAE of the vehicle emissions sourced was much higher than that of the biomass burning sourced (Hu et al., 2017). It is urgent to evaluate the influence of vehicle emission of highway on the MAE changes in surrounding areas to assess regional radiation forcing.

In this study, online and offline measurements of aerosol chemical composition and light absorption were conducted in Nanjing, a mega-city located in the Yangtze River Delta (YRD) region in eastern China, with a high level of BC emissions (Zhang et al., 2013). The primary objectives of this study were 1) to investigate the discrepancy in MAE values by different sampling modes and thermal/optical analysis methods and 2) to evaluate the impact of vehicle emission of highway on MAE variation through simultaneous observation by two sites.

MATERIALS AND METHODS

Measurement Sites and Aerosol Sample Collection

Ambient aerosol samples were collected at the School of the Environment Nanjing University (SE) and the Station for Observing Regional Processes of the Earth System (SORPES) (32.07°N, 118.57°E), and the locations of the two sites are shown in **Supplementary Figure S1** in the Supplement. The SE site was on the School of the Environment building in the Xianlin Campus of Nanjing University in eastern Nanjing (25 m above the ground level). The SORPES site was on the top of a small hill (40 m above sea level) in the Xianlin Campus, and the site is 390 m to the east of the SE site. SE and SORPES were about 400 and 790 m away from the G25 highway, respectively.

All offline aerosol samples were collected with $PM_{2.5}$ samplers (TH-150C, Tianhong, China) at a flow rate of 100 L/min. A total of 86 and 20 (24-h cycle starting at 9:00 a.m.) $PM_{2.5}$ samples were obtained at SE and SORPES, from November 2015 to October 2016, respectively. Specifically, 86 daily $PM_{2.5}$ samples from November 2015 to October 2016 at SE were used in the comparison of the MAE values by different sampling and temperature protocols. The 20 daily $PM_{2.5}$ samples from September to October 2016 at SE and the 20 daily samples with the same time at SORPES were used to study the influence of vehicle emission of highway on MAE values. Besides, hourly carbonaceous aerosol (OC and EC) was simultaneously sampled by semi-continuous carbon analyzer (Model-4, Sunset Lab, USA) with a small flow of 8 L/min, and there were two modes in online sampling: with and without using denuder.

Measurements and Carbonaceous Components

The concentrations and light absorption parameters of carbonaceous components were measured by the semi-continuous carbon analyzer using the NIOSH protocol. There were some pyrolized carbon (PC) formed from OC converted to EC and, thus, led the calculated deviation. The He–Ne diode laser beam at 678 nm through the filter was taken for charring correction. The split point between OC and EC was defined by thermal optical transmittance (TOT), the carbon before the split point was considered as OC, and the rest as EC (Wu et al.,

TABLE 1 | Temperature programs (T) and residence time (RT) of the five protocols (NIOSH, NIOSH580, NIOSH5040, Rt-quartz, and IMPROVE-A).

Step	Carrier gas	NIOSH		NIOSH580		NIOSH5040		RT-quart		IMPROVA-A	
		T (°C)	RT(s)	T (°C)	RT(s)	T (°C)	RT(s)	T (°C)	RT(s)	T (°C)	RT(s)
OC1	He	310	70	310	70	310	70	600	95	140	150–580
OC2	He	480	60	480	60	480	60	840	90	280	150–580
OC3	He	615	60	580	150	615	60	n.a	n.a	480	150–580
OC4	He	840	90	n.a	n.a	840	100	n.a	n.a	580	150–580
EC1	He/O_2[a]	550	35	550	35	550	40	550	35	580	150–580
EC2	He/O_2[a]	850	105	850	105	625	45	650	45	740	150–580
EC3	He/O_2[a]	n.a	n.a	n.a	n.a	700	45	870	115	840	150–580
EC4	He/O_2[a]	n.a	n.a	n.a	n.a	775	45	n.a	n.a	n.a	n.a
EC5	He/O_2[a]	n.a	n.a	n.a	n.a	850	120	n.a	n.a	n.a	n.a

[a]*Actual gas composition: 98% He + 2% O_2.*

2012). For offline sample analysis on the carbon analyzer, a punch of 1.25 cm^2 for each filter sample for measurement and four protocols (including NIOSH, NIOSH5040, NIOSH580, and RT-quartz) were adopted for carbon analysis. On a DRI analyzer, a filter punch of 0.5 cm^2 was used, and IMPROVE protocol was conducted (monitored at 632 nm). All the filter samples were charring corrected by TOT transmittance to eliminate the charring correction uncertainty by the two instruments. The detailed temperature programs of the five protocols are presented in **Table 1**. The major differences between the five protocols were as follows: 1) The maximum temperature in the He stage reaches 840°C in the NIOSH, NIOSH5040, and RT-quartz protocols, whereas 580°C in the NIOSH580 and IMPROVE-A protocols; 2) The residence time (RT) was fixed for each temperature step in four NIOSH-derived protocols, while the RT of each temperature step was variable in IMPROVE-A, and the resulting RT of the IMPROVE-A protocol is over two times larger than that of the NIOSH-derived protocols.

Determination of Mass Absorption Efficiency

The MAE of EC was estimated from the optical attenuation (ATN); ATN can be calculated based on Beer–Lambert's law as follows:

$$ATN = \ln\left(\frac{I_0}{I}\right) \tag{1}$$

where I_0 and I are the intensity of the incident light and the transmitted light through the filter substrate and aerosols, respectively. The MAE is then calculated as:

$$MAE\left(m^2/g\right) = \frac{ATN}{EC \times C \times R(ATN)} \times \frac{A}{V} = \frac{ATN}{EC_S \times C \times R(ATN)} \tag{2}$$

where EC_s is the elemental carbon loading on the filter (μg/cm^2), A and V are the filter area (cm^2) and sampled air volume (m^3), respectively, And C and R (ATN) are the two empirical factors for correcting the artifacts due to multiple scattering and shadowing effects, respectively. Weingartner et al. (2003) estimated R (ATN) based on the aethalometer data:

$$R(ATN) = \left(\frac{1}{f} - 1\right) \times \frac{\ln(ATN) - \ln(0.1)}{\ln(0.5) - \ln(0.1)} + 1 \tag{3}$$

Ram and Sarin calculated the shadowing effects by setting f as 1.103 during wintertime and 1.114 for the rest of the seasons (Ram and Sarin, 2009). In the present study, an empirical factor of 2.14 was adopted in the calculation since comparable ATN values were reported between the aethalometer and Sunset carbon analyzer (Cheng et al., 2011a; Ram and Sarin, 2009). The R (ATN) value was varied depending on seasonal demand, and more details about the R (ATN) calculation can be found in our previous publication (Chen et al., 2019).

Estimation of Secondary Organic Carbon

The concentrations of secondary organic carbon (SOC) at the two sites were estimated by using the EC tracer method (Turpin and Huntzicker, 1991; Lim and Turpin, 2002).

$$SOC = OC - EC \times (OC/EC)_{primary} \tag{4}$$

where OC and EC are the OC and EC concentrations, respectively; $(OC/EC)_{primary}$ is the ratio of primary OC and EC emissions. In this study, the correlation coefficient between EC and OC at 0.95 was taken as a threshold, i.e., the hourly OC and EC concentrations with correlation coefficient larger than 0.95 were selected to calculate the $(OC/EC)_{pri}$.

RESULTS AND DISCUSSION

Inter-Sampling Comparison of Mass Absorption Efficiency

The main differences between offline and online sampling modes were the denuder used in online and the large flow in offline sampling. The online sampling generally equipped with a carbon impregnated multichannel parallel plate diffusion denuder to reduce positive artifact in OC measurement. The comparison of MAE estimated by online with denuder and offline samplings is presented in **Figure 1A**, poor correlation was found between MAE values by the two samplings (R^2 = 0.33), the mean MAE value of offline sampling was estimated at 9.9 m^2/g and was 26.9% larger than that of online sampling with a denuder (7.8 m^2/g)

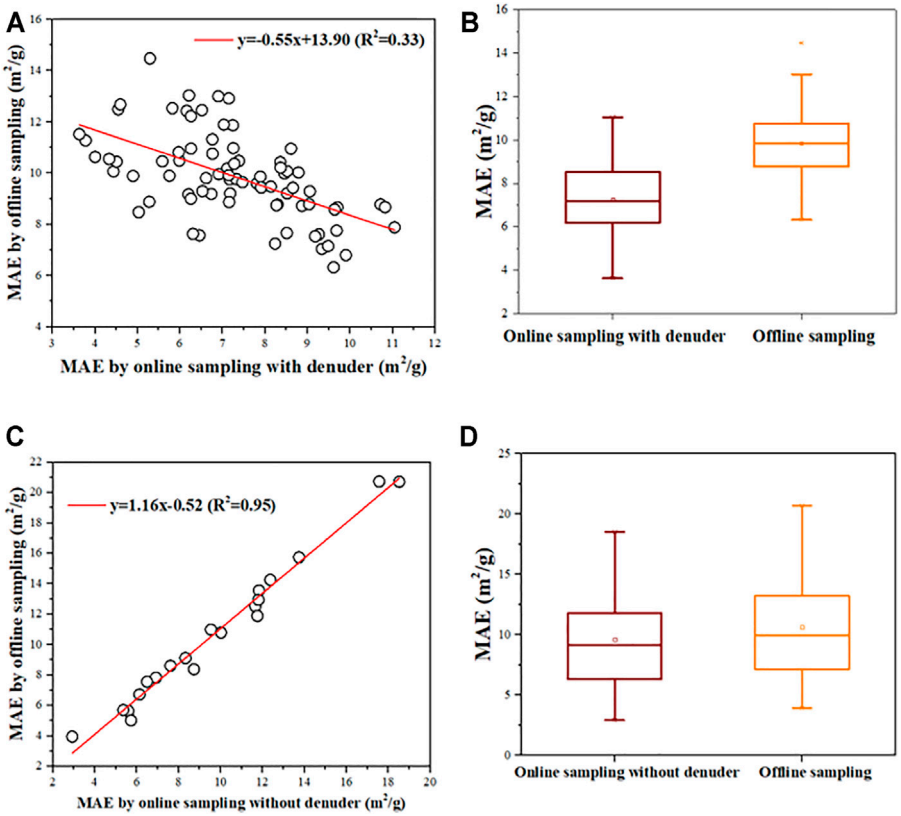

FIGURE 1 | Comparison of mass absorption efficiency (MAE) values between offline and online samplings. **(A)** The correlation between MAE by offline sampling and that by online sampling with a denuder. **(B)** Box plots of MAE by offline sampling and that by online sampling with a denuder. **(C)** The correlation between MAE by offline sampling and that by online sampling without a denuder. **(D)** Box plots of MAE by offline sampling and that by online sampling without a denuder.

(**Figure 1B**). Another 20 ambient samples by online sampling without a denuder were collected in June 2016 at SE. As shown in **Figure 1C**, good correlation was found between MAE values by online sampling without a denuder and that by offline sampling (R^2 = 0.95), and the mean MAE of offline was 10.4% larger than that by online without a denuder (**Figure 1D**). These results indicated that the use of the denuder would largely underestimate the determination of MAE. According to the relationship between the sampling flow and the effective filter area of the two sampling modes, the result showed that the EC mass of offline sampling should be 7.11 times than that of online mode. As shown in **Supplementary Figure S2A** in the supplementary material, the slope of offline EC mass to that of online sampling with a denuder was 8.45, and 19% higher than the predicted value, indicating that EC mass probably is lost by online sampling.

As shown in **Supplementary Figure S2B**, good correlation (R^2 = 1) was found between the EC mass measured by offline sampling and that by online sampling without a denuder, indicating the consistency measurements between the two samplings. Compared with the previous result, the overestimation rate was reduced to 16%, indicating that losing

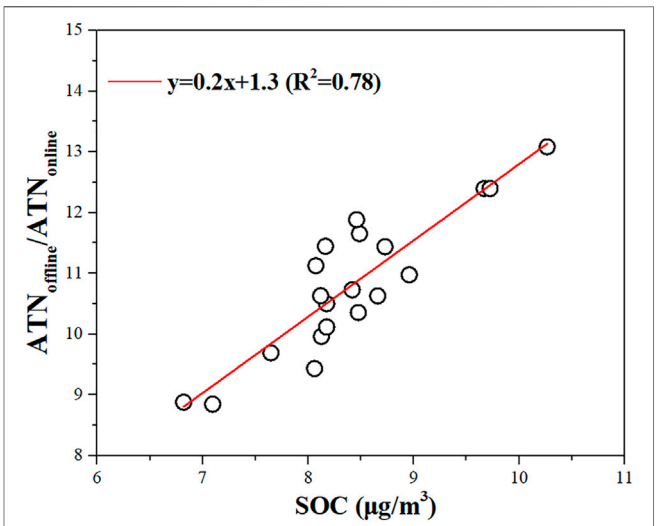

FIGURE 2 | The relationship between secondary organic carbon (SOC) and the ratio of light attenuation (ATN) by offline sampling to that by online sampling without a denuder ($ATN_{offline}/ATN_{online}$).

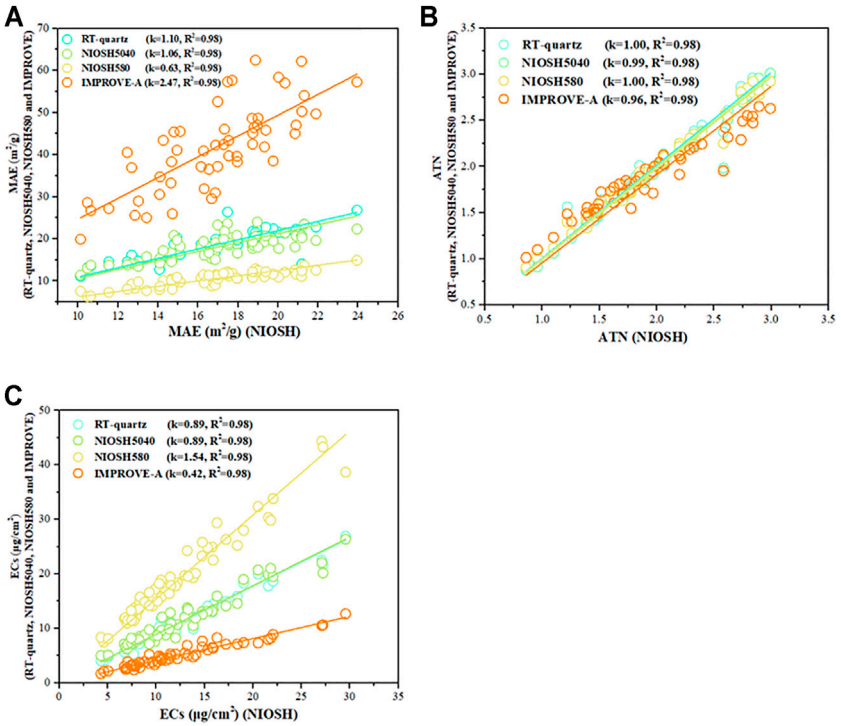

FIGURE 3 | Mass absorption efficiency (MAE), optical attenuation (ATN), and elemental carbon (EC) mass by the National Institute for Occupational Safety and Health (NIOSH) protocol compared with those by RT-quartz, NIOSH5040, NIOSH580, and Interagency Monitoring of Protected Visual Environments (IMPROVE)-A protocols. **(A)** Comparison of MAE by different temperature protocols. **(B)** Comparison of light attenuation (ATN) by different temperature protocols. **(C)** Comparison of EC mass by different temperature protocols.

EC in online sampling with a denuder was about 3%, whereas a large difference in EC determination between the two samplings still existed. These results indicated that a small flow in online sampling was the main cause for the large loss of EC collection.

In the actual atmospheric environment, the formation of SOA from volatile organic compounds (VOCs) would further enhance the light absorption capacity of particles, and thereby elevating the ATN (Cheng et al., 2017; Chen et al., 2019). The relationship between SOC and the ratio of ATN by offline sampling to that by online sampling without a denuder ($ATN_{offline}/ATN_{online}$) is presented in **Figure 2**. Good correlation was found between SOC concentration and $ATN_{offline}/ATN_{online}$ (R^2 = 0.88), and the $ATN_{offline}/ATN_{online}$ increased with the elevated SOC, indicating that the large difference in ATN by online and offline sampling modes appeared in the high loading of SOA. These results implied that the difference in MAEs by the two types of sampling was greatly influenced by SOA pollution.

The Impact of Temperature Protocol on Mass Absorption Efficiency

To investigate the impact of temperature protocol on MAE, four NIOSH-derived protocols (NIOSH, NIOSH580, NIOSH5040, and Rt-quartz) and one IMPROVE-A protocol were applied to measure the light absorption and EC mass. In order to eliminate the deviation caused by different charring correction methods, all the five protocols were applied with thermal optical transmittance (TOT) to charring correction. As shown in **Figure 3A**, strong correlations between MAEs by four protocols (RT-quartz, NIOSH5040, NIOSH580, and IMPROVE) with MAE by NIOSH were found (R^2 > 0.98), indicating that MAEs measured by these protocols were consistent in the overall trend. The slopes of MAEs estimated by Rt-quartz and NIOSH5040 to NIOSH protocol were both close to 1, indicating little difference in MAE estimation by the three protocols. The MAE measured by IMPROVE-A was 147% larger than the MAE by NIOSH, and the MAE by NIOSH580 was 37% lower than that by NIOSH, indicating the large difference in the determination of MAE by IMPROVE-A, NIOSH, and NIOSH580. The slopes of ATN values by the four protocols versus NIOSH are presented in **Figure 3B**; the deviations of the five protocols on ATN determination were within 5%, indicating the consistency in ATN determinations by the five protocols. A slight difference was found in ATN values by NIOSH and IMPROVE-A protocols, and this probably is due to the different wavelengths used in the two protocols. A previous study in Beijing found that ATN mainly displayed strong wavelength dependence (Cheng et al., 2012). NIOSH and IMPROVE-A protocols were conducted by Sunset and DRI thermal/optical carbon analyzers, which were monitored at 678 and 632 nm, respectively. Thus, the main reason for the

TABLE 2 | The mass concentrations of organic carbon (OC), elemental carbon (EC) and secondary organic carbon (SOC), the ratio of SOC to OC (SOC/OC), the mass absorption efficiency (MAE) and optical attenuation (ATN) at the School of Environment (SE) and at the Station for Observing Regional Processes of the Earth System (SORPES) in May and June of 2016.

Sites	OC	EC	SOC	SOC/OC	MAE	ATN
	(μg/m^3)	(μg/m^3)	(μg/m^3)	(%)	(m^2/g)	
SE	10.92 ± 4.02	2.73 ± 0.91	2.41 ± 1.77	22.12 ± 17.32	9.53 ± 2.52	1.28 ± 0.34
SORPES	9.58 ± 3.60	2.21 ± 0.62	2.34 ± 1.80	23.33 ± 16.32	10.41 ± 2.72	1.39 ± 0.36

difference in MAE estimation by different protocols was the discrepancy in EC determination.

As shown in **Figure 3C**, the EC mass measured by NIOSH580 was 54% greater than that by NIOSH protocol, the EC mass measured by IMPROVE-A was 58% lower than that by NIOSH protocol. There was little difference in the EC mass measured by NIOSH, NIOSH5040, and Rt-quartz. According to a previous study (Cheng et al., 2011b), the five protocols differed mainly with respect to temperature protocol such as peak inert mode temperature (T_{peak}) and residence time at each plateau. To explore the influence of T_{peak} on the determination of EC mass, NIOSH580 protocol was developed based on NIOSH in this study, and the main difference between the two protocols was that the temperature gradient of NIOSH, which was higher than 580°C in inert mode was changed to 580°C in NIOSH580, and the other temperature gradients remained constant (as shown in **Supplementary Figure S3**). As shown in **Figure 3C** and **Supplementary Figure S4**, no significant differences were found in TC masses measured by the two protocols, whereas EC of NIOSH580 was 54% greater than that of NIOSH. The pyrolysis carbon mass of NIOSH580 was 7.8 ± 2.3 μg, which was about 36% lower than that of NIOSH, and average split time of NIOSH (410 ± 20 s) was about 25 s longer than that of NIOSH580 (385 ± 16 s). The low peak inert mode temperature in NIOSH580 led to a small amount of pyrolysis carbon, resulting in overestimation of EC and thereby underestimation of MAE. Besides T_{peak}, residence time (RT) was another important parameter of protocol. According to **Supplementary Figure S5**, the RT of peak inert mode in IMPROVE-A was 870s, about three times longer than that in NIOSH. Cheng et al. (2011b) suggested that prolonging the residence time could considerably enhance carbon evolution. Much longer residence time in the inert mode of IMPROVE-A promoted to decrease the estimated EC and eventually overestimated MAE.

The Impact of Highway Vehicle Emission on Mass Absorption Efficiency

Further study on the influence of vehicle emission on MAE was conducted at SE and SORPES sites. As shown in **Table2**, the MAE of SE was estimated at 9.5 m^2/g, which was 8.5% lower than that of SORPES, and the result showed that the mean MAE value increased by 2.2% with an increment distance of 100 m away from the G25 highway. The discrepancy in MAE values between the two sites was expected to be relevant with the dry deposition of EC from vehicle emission and the lensing effect by SOA coating.

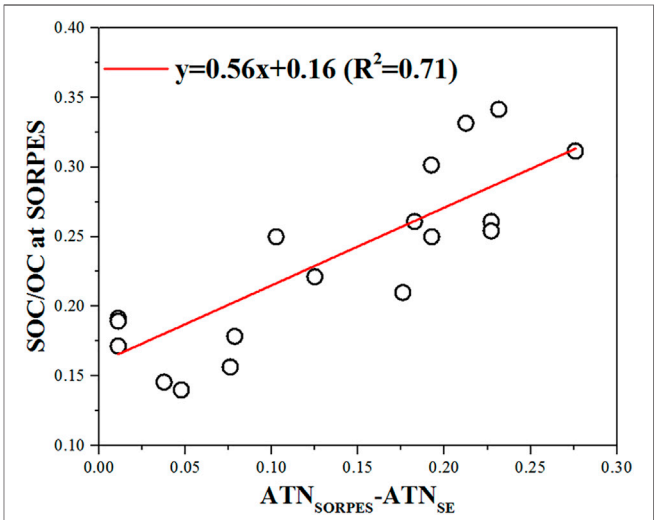

FIGURE 4 | Correlation between the changes in light attenuation (ATN_{SORPES}-ATN_{SE}) and the ratios of secondary organic carbon (SOC) to organic carbon (OC) (SOC/OC) at the Station for Observing Regional Processes of the Earth System (SORPES).

According to the *Materials and methods* section, SE is 390 m closer to the highway road than SORPES. Except for the influence of vehicle emission, there is no obvious emission sources nearby. According to our previous study on the fractions of vehicles in the G25 highway with recording by real-time camera, a strong correlation between EC concentration and diesel vehicle fraction was found (Chen et al., 2017d), which indicated that diesel vehicle emission was the dominate source of EC at SE and SORPES sites. The concentrations of EC at SE and SORPES are presented in **Table 2**. The EC concentration at SE was 2.7 μg/m^3, about 20% greater than that at SORPES (2.2 μg/m^3). Since EC was only produced from primary combustion sources, the decreased EC at SORPES was mainly due to dry deposition. Without considering the vertical diffusion of EC concentration, the mean EC concentration was calculated to decrease by 0.13 μg/m^3 with an increment distance of 100 m. Compared with the MAE of aged EC, the MAE of fresh EC emitted by the vehicle was closer to that of pure EC (Cui et al., 2015). Thus, low MAE at SE was mainly affected by the primary emission of diesel vehicle.

As one of the main pollutants exhausted by vehicle, OC of SE (11.0 μg/m^3) was 15% greater than that at SORPES (9.5 μg/m^3) (**Table 2**). ATN changed less than OC and EC concentrations; ATN at SE was only 8.5% greater than that at SORPES. The result can be attributed to an elevated SOA concentration at SORPES.

Besides primary emission, OC could also be generated by gas-to-particle partition processes from VOCs. A previous study indicated that SORPES suffered SOA formation process from eastern YRD (Sun et al., 2020). Based on the EC tracer method, SOC concentrations at the two sites were estimated. Higher fraction of SOC in OC at SORPES than that at SE (**Table 2**) indicates the elevated secondary organic pollution. Moreover, the difference in ATN of the two sites showed stronger correlation with SOC/OC at SORPES (**Figure 4**), indicating that the lensing effect by SOC coating was another important factor affecting the high MAE value at SORPES. These results indicated that a low MAE value of EC around the highway was mainly affected by the emission of diesel vehicle with a high content of EC. With the increasing distance from the highway, the MAE value increased due to the factors such as the lensing effect by SOA coating.

CONCLUSION

The MAE of EC was investigated at two sites, which are adjacent to a highway in Nanjing, a typical polluted city with complicated sources of ambient aerosols. Compared with MAE by online sampling with a denuder, MAE of online sampling without a denuder was much closer to the MAE of offline sampling, implying that the use of the denuder would bring large uncertainty in MAE estimation. A small flow in online sampling caused the large loss of EC collection. Compared with MAE of offline sampling, a lower MAE of online sampling was attributed to the decreased ATN from the losing EC, especially during high SOA concentration. In the comparison of MAE estimated by the five temperature protocols, large differences were found among IMPROVE-A, NIOSH, and NIOSH580 protocols. The result indicated that the significant difference in EC mass measurements was the main factor causing the change in MAE. The low peak inert mode temperature in NIOSH580 led to a small amount of pyrolysis organic carbon, resulting in overestimation of EC and, thereby, underestimation of MAE. Long residence time can enhance carbon evolution, and much longer residence time in the inert mode of IMPROVE-A caused the underestimation of EC concentration and eventually to the overestimation of MAE. In order to effectively compare the spatial and temporal variations in EC concentration and its light absorption, it is recommended to use offline sampling method and NIOSH-type protocols (NIOSH, NIOSH5040, or Rt-quartz) in future work. Based on the simultaneous observation at SE and SORPES, we found that MAE of SE was 8.5% lower than that of SORPES, and the mean MAE value was calculated to increase by 2.2% with an increment distance of 100 m. The ATN and the concentrations of carbonaceous components (OC, EC, and SOC) at the two sites were estimated, and the results indicated that EC dry deposition and the lensing effect by SOC coating were the main causes for the high MAE values at SORPES site, which was farther away from the highway.

DATA AVAILABILITY STATEMENT

The raw data supporting the conclusion of this article will be made available by the authors, without undue reservation.

AUTHOR CONTRIBUTIONS

DC handled the methodology, investigation, data analyses, and writing of the original draft. MG and ZA took part in the investigation, writing the original draft, and resource acquisition. QZ, SX, and LL performed the data analyses and were responsible for project administration and funding acquisition.

FUNDING

For support, we thank the Jiangsu Provincial Fund on $PM_{2.5}$ and O_3 pollution mitigation (No. 2019023), Jiangsu Planned Projects for Postdoctoral Daily Funds (No. 2020Z362), National Key Research and Development Project (No. 2018YFC0213803), Natural Science Foundation of the Jiangsu Higher Education Institutions (No. 19KJB180003), and the Program B for Outstanding Candidates of Nanjing University (Nos. 201702B058 and 201702B056).

SUPPLEMENTARY MATERIAL

The Supplementary Material for this article can be found online at: https://www.frontiersin.org/articles/10.3389/fenvs.2021.812039/full#supplementary-material

REFERENCES

Abdull, N., Yoneda, M., and Shimada, Y. (2020). Traffic Characteristics and Pollutant Emission from Road Transport in Urban Area. *Air Qual. Atmosphere Health* 13, 7655. doi:10.1007/s11869-020-00830-w

Bond, T. C., and Bergstrom, R. W. (2006). Light Absorption by Carbonaceous Particles: An Investigative Review. *Aerosol Sci. Tech.* 40, 27–67. doi:10.1080/02786820500421521

Bond, T. C., Doherty, S. J., Fahey, D. W., Forster, P. M., Berntsen, T., DeAngelo, B. J., et al. (2013). Bounding the Role of Black Carbon in the Climate System: a Scientific Assessment. *J. Geophys. Res. Atmos.* 118, 5380–5552. doi:10.1002/jgrd.50171

Chen, B., Bai, Z., Cui, X., Chen, J., Andersson, A., and Gustafsson, Ö. (2017a). Light Absorption Enhancement of Black Carbon from Urban Haze in Northern China winter. *Environ. Pollut.* 221, 418–426. doi:10.1016/j.envpol.2016.12.004

Chen, D., Cui, H., Zhao, Y., Yin, L., Lu, Y., and Wang, Q. (2017b). A Two-Year Study of Carbonaceous Aerosols in Ambient PM2.5 at a Regional Background Site for Western Yangtze River Delta, China. *Atmos. Res.* 183, 351–361. doi:10.1016/j.atmosres.2016.09.004

Chen, D., Zhao, Y., Lyu, R., Wu, R., Dai, L., Zhao, Y., et al. (2019). Seasonal and Spatial Variations of Optical Properties of Light Absorbing Carbon and its Influencing Factors in a Typical Polluted City in Yangtze River Delta, China. *Atmos. Environ.* 199, 45–54. doi:10.1016/j.atmosenv.2018.11.022

Cheng, Y., Duan, F.-k., He, K.-b., Du, Z.-y., Zheng, M., and Ma, Y.-l. (2012). Intercomparison of thermal-optical Method with Different Temperature

Protocols: Implications from Source Samples and Solvent Extraction. *Atmos. Environ.* 61, 453–462. doi:10.1016/j.atmosenv.2012.07.066

Cheng, Y., Duan, F.-k., He, K.-b., Zheng, M., Du, Z.-y., Ma, Y.-l., et al. (2011b). Intercomparison of Thermal-Optical Methods for the Determination of Organic and Elemental Carbon: Influences of Aerosol Composition and Implications. *Environ. Sci. Technol.* 45, 10117–10123. doi:10.1021/es202649g

Cheng, Y., He, K.-b., Engling, G., Weber, R., Liu, J.-m., Du, Z.-y., et al. (2017). Brown and Black Carbon in Beijing Aerosol: Implications for the Effects of Brown Coating on Light Absorption by Black Carbon. *Sci. Total Environ.* 599-600, 1047–1055. doi:10.1016/j.scitotenv.2017.05.061

Cheng, Y., He, K. B., Zheng, M., and Duan, F. K. (2011a). Mass Absorption Efficiency of Elemental Carbon and Water-Soluble Organic Carbon in Beijing, China. *Atmos. Chem. Phys.* 11, 24727–24764. doi:10.5194/acp-11-11497-2011

Cui, H., Mao, P., Zhao, Y., Nielsen, C. P., and Zhang, J. (2015). Patterns in Atmospheric Carbonaceous Aerosols in China: Emission Estimates and Observed Concentrations. *Atmos. Chem. Phys.* 15, 8657–8678. doi:10.5194/acp-15-8657-2015

Han, T., Qiao, L., Zhou, M., Qu, Y., Du, J., Liu, X., et al. (2015). Chemical and Optical Properties of Aerosols and Their Interrelationship in winter in the Megacity Shanghai of China. *J. Environ. Sci.* 27, 59–69. doi:10.1016/j.jes.2014.04.018

Hu, Z., Kang, S., Li, C., Yan, F., Chen, P., Gao, S., et al. (2017). Light Absorption of Biomass Burning and Vehicle Emission-Sourced Carbonaceous Aerosols of the Tibetan Plateau. *Environ. Sci. Pollut. Res.* 24, 15369–15378. doi:10.1007/s11356-017-9077-3

Jacobson, M. Z. (2001). Strong Radiative Heating Due to the Mixing State of Black Carbon in Atmospheric Aerosols. *Nature* 409, 695–697. doi:10.1038/35055518

Lim, H.-J., and Turpin, B. J. (2002). Origins of Primary and Secondary Organic Aerosol in Atlanta: Results of Time-Resolved Measurements during the Atlanta Supersite experiment. *Environ. Sci. Technol.* 36, 4489–4496. doi:10.1021/es0206487

Liu, D., Whitehead, J., Alfarra, M. R., Reyes-Villegas, E., Spracklen, D. V., Reddington, C. L., et al. (2017). Black-carbon Absorption Enhancement in the Atmosphere Determined by Particle Mixing State. *Nat. Geosci* 10, 184–188. doi:10.1038/ngeo2901

Shen, G., Chen, Y., Wei, S., Fu, X., Zhu, Y., and Tao, S. (2013). Mass Absorption Efficiency of Elemental Carbon for Source Samples from Residential Biomass and Coal Combustions. *Atmos. Environ.* 79, 79–84. doi:10.1016/j.atmosenv.2013.05.082

Sun, J., Xie, C., Xu, W., Chen, C., Ma, N., Xu, W., et al. (2021). Light Absorption of Black Carbon and Brown Carbon in winter in North China Plain: Comparisons between Urban and Rural Sites. *Sci. Total Environ.* 770, 144821. doi:10.1016/j.scitotenv.2020.144821

Sun, P., Nie, W., Wang, T., Chi, X., Huang, X., Xu, Z., et al. (2020). Impact of Air Transport and Secondary Formation on Haze Pollution in the Yangtze River Delta: *In Situ* Online Observations in Shanghai and Nanjing. *Atmos. Environ.* 225, 117350. doi:10.1016/j.atmosenv.2020.117350

Turpin, B. J., and Huntzicker, J. J. (1991). Secondary Formation of Organic Aerosol in the Los Angeles basin: A Descriptive Analysis of Organic and Elemental Carbon Concentrations. *Atmos. Environ. A. Gen. Top.* 25, 207–215. doi:10.1016/0960-1686(91)90291-e

Wang, Q., Huang, R.-J., Cao, J., Han, Y., Wang, G., Li, G., et al. (2014). Mixing State of Black Carbon Aerosol in a Heavily Polluted Urban Area of China: Implications for Light Absorption Enhancement. *Aerosol Sci. Tech.* 48, 689–697. doi:10.1080/02786826.2014.917758

Wang, T., Zhao, G., Tan, T., Yu, Y., Tang, R., Dong, H., et al. (2021). Effects of Biomass Burning and Photochemical Oxidation on the Black Carbon Mixing State and Light Absorption in Summer Season. *Atmos. Environ.* 248, 118230. doi:10.1016/j.atmosenv.2021.118230

Watson, J. G., Chow, J. C., and Chen, L.-W. A. (2005). Summary of Organic and Elemental Carbon/black Carbon Analysis Methods and Intercomparisons. *Aerosol Air Qual. Res.* 5, 65–102. doi:10.4209/aaqr.2005.06.0006

Wen, Y., Wang, H., Larson, T., Kelp, M., Zhang, S., Wu, Y., et al. (2019). On-highway Vehicle Emission Factors, and Spatial Patterns, Based on mobile Monitoring and Absolute Principal Component Score. *Sci. Total Environ.* 676, 242–251. doi:10.1016/j.scitotenv.2019.04.185

Wu, C., Ng, W. M., Huang, J., Wu, D., and Yu, J. Z. (2012). Determination of Elemental and Organic Carbon in PM2.5in the Pearl River Delta Region: Inter-instrument (Sunset vs. DRI Model 2001 Thermal/Optical Carbon Analyzer) and Inter-protocol Comparisons (IMPROVE vs. ACE-Asia Protocol). *Aerosol Sci. Tech.* 46, 610–621. doi:10.1080/02786826.2011.649313

Zhang, N., Qin, Y., and Xie, S. (2013). Spatial Distribution of Black Carbon Emissions in China. *Chin. Sci. Bull.* 58, 3830–3839. doi:10.1007/s11434-013-5820-4

Zhao, X., Zhao, Y., Chen, D., Li, C., and Zhang, J. (2019). Top-down Estimate of Black Carbon Emissions for City Clusters Using Ground Observations: a Case Study in Southern Jiangsu, China. *Atmos. Chem. Phys.* 19, 2095–2113. doi:10.5194/acp-19-2095-2019

Zhao, Z., Wang, Q., Xu, B., Shen, Z., Huang, R., Zhu, C., et al. (2017). Black Carbon Aerosol and its Radiative Impact at a High-Altitude Remote Site on the southeastern Tibet Plateau. *J. Geophys. Res. Atmos.* 122, 5515–5530. doi:10.1002/2016jd026032

Conflict of Interest: The authors declare that the research was conducted in the absence of any commercial or financial relationships that could be construed as a potential conflict of interest.

Publisher's Note: All claims expressed in this article are solely those of the authors and do not necessarily represent those of their affiliated organizations, or those of the publisher, the editors, and the reviewers. Any product that may be evaluated in this article, or claim that may be made by its manufacturer, is not guaranteed nor endorsed by the publisher.